Creep of backfill geogrid reinforcement for retaining walls

F. Navarrete
Florida Atlantic University, Boca Raton, Florida, U.S.A.

Consejo Nacional de Ciencia y Tecnologia, Mexico, D.F. Mexico

D. V. Reddy
Florida Atlantic University, Boca Raton, Florida, U.S.A.

P. Lai
Florida Department of Transportation (FDOT), Tallahassee, Florida, U.S.A.

Keywords: Creep, Geogrids, Reinforcement, Walls

ABSTRACT: This study addresses the creep and creep-rupture investigation for two types of geogrids: High Density Polyethylene (HDPE) and Polyethylene Terephthalate (PET). Accelerated exposure was used, with super-ambient temperatures for different simulated exposure conditions, and soil water related to the soil conditions in Florida. The temperatures were: 30° C, 45° C, 55° C, and 65° C; with submergence in the following groundwater-simulating solutions: HDPE specimens - calcareous (pH 9.0), phosphate (pH 4.5), limerock, seawater, and freshwater for PET specimens only. The load levels were 30%, 40%, 50% of the ultimate load value. Elongations were measured at 30 seconds, 1, 2, 4, 6, 8, 15, 30, 75 minutes, 3, 7 hours, and every 24 hours, up to 10,000 hours. It was observed that HDPE geogrids undergo larger creep than PET geogrids. The different exposures do not play an important role in the rate of creep. Creep rupture occurred in all the HDPE specimens exposed to 50% of the ultimate load, and for the specimens exposed to 40% of the ultimate load, and to 55° C and 65° C temperatures. The PET specimens did not experience creep rupture except for two specimens; for these two cases the rupture was attributed to either defects in the specimens or defective clamping.

1 INTRODUCTION

The main polymers currently used for reinforcement include polypropylene (PP), polyester terephthalate (PET), and polyethylene (PE). Geogrids were first introduced into North America in the early 1980's. The ASTM D5262 (1992) defines a geogrid as "a geosynthetic formed by a rectangular network of integrally connected elements with apertures greater than 6.35mm (1/4 in.) to allow interlocking with the surrounding soil, rock, earth, and other surrounding materials to function primarily as a reinforcement". Geogrids are produced for biaxial and uniaxial load-carrying configurations.

Due to the relatively short experience with these polymeric materials, there are uncertainties regarding their durability, with respect to retainment of the design properties after being subjected to construction stresses and exposed to in-soil environments over the expected design life. Potential degradation of polymeric reinforcement, with time, will depend on the characteristics of a specific polymer, configuration, and the environment to which it is exposed. This dictates the need for more research in this area. If geogrids have to be used as an alternative to steel reinforcement to overcome the corrosion problem, their performance has to be established based on laboratory and field testing for site specific conditions, e.g. high water tables and temperatures ranging between 27^{o} C to 38^{o} C in Florida.

1.1 *HDPE Geogrids*

HDPE is the acronym for High Density Polyethylene, The uniaxial HDPE geogrids used in this research are manufactured by stretching a punched sheet of extruded HDPE in one direction, under carefully controlled conditions. This process aligns the polymer's long-chain molecules in the direction of drawing, and results in a product with high one-directional tensile strength and modulus.

1.2 *PET Geogrids*

PET is the acronym for Polyester Terephthalate. PET geogrids are made of polyester multifilament yarns, which are interlocked by weaving to create a stable network, such that the yarns retain their relative position. Compared to HDPE, PET is more flexible in bending and exhibits a relatively lower junction strength.

1.3 *Creep and Creep Rupture*

Creep is simply the viscoelastic response of the reinforcement due to a sustained load. It results in time-dependent deformation, which may continue to occur as long as the reinforcement is loaded. It is of primary importance in the design of polymeric reinforced structures, Allen (1991). Geosynthetic structure tends to dominate primary creep, whereas the polymer material tends to dominate secondary and tertiary creep, Allen, Bell, and Vinson (1983). Soil confinement tends to restrict the movement of individual filaments, preventing their realignment in the direction of load, thereby substantially reducing the magnitude of geosynthetic macrostructure creep i.e., primary creep, McGown, Andrews, and Kabir (1982). Koerner et al. (1980) postulated that the creep behavior of the soil influences the creep behavior of the geosynthetic. Chemical aging of geosynthetics is the result of both soil environmental factors and the polymer chemical structure. In general, chemical aging can affect creep at relatively high temperatures, as those encountered in Florida, with moderate high moisture conditions in soils which are chemically active.

Creep-rupture is expressed in terms of decreasing life with increasing stress and temperature, and the transition from ductile to brittle behavior. It is important to identify the "failure time transition" point in the creep-rupture plot for realistic estimation of life. Figure 1 shows the creep rupture behavior for a semi-crystalline polymer.

Chemical aging can affect creep and creep rupture at relatively high temperatures, as those encountered in Florida, with moderate high moisture conditions in soils, which are chemically active.

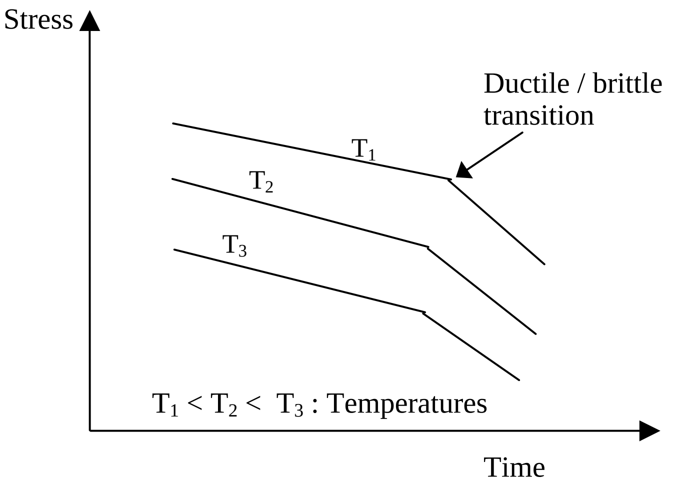

Figure 1. Creep-rupture behavior for a semi-crystalline polymer. Ahn et al. (1998)

2 EXPERIMENTAL INVESTIGATION

To simulate different exposure conditions, 20 tanks were fabricated with super-ambient temperatures for different simulated exposure conditions, and soil water related to the soil conditions in Florida.

The temperatures were 30° C, 35° C, 45° C, 55° C and 65° C, with submergence in the following groundwater-simulating solutions:

HDPE specimens:

- Calcareous (pH 9.0)
- Phosphate (pH 4.5)
- Limerock
- Seawater

PET specimens

- Calcareous (pH 9.0)
- Phosphate (pH 4.5)
- Limerock
- Seawater
- Freshwater

The load levels were: 30 %, 40 % and 50 % of the ultimate load.

The results are presented for creep strain and creep rupture tests on both HDPE and PET test specimens.

The values of creep strain were plotted for each of the two specimen types categorized as: "Specimen Set I" and "Specimen Set II". Each graph corresponds to a geogrid type, specimen set, temperature and load level, including all environmental exposures. Regression analysis was carried out for each specimen.

From the creep strain, it can be seen that PET geogrids resist creep strain better than HDPE ones at similar temperatures and load levels, Figures 2 and 3.

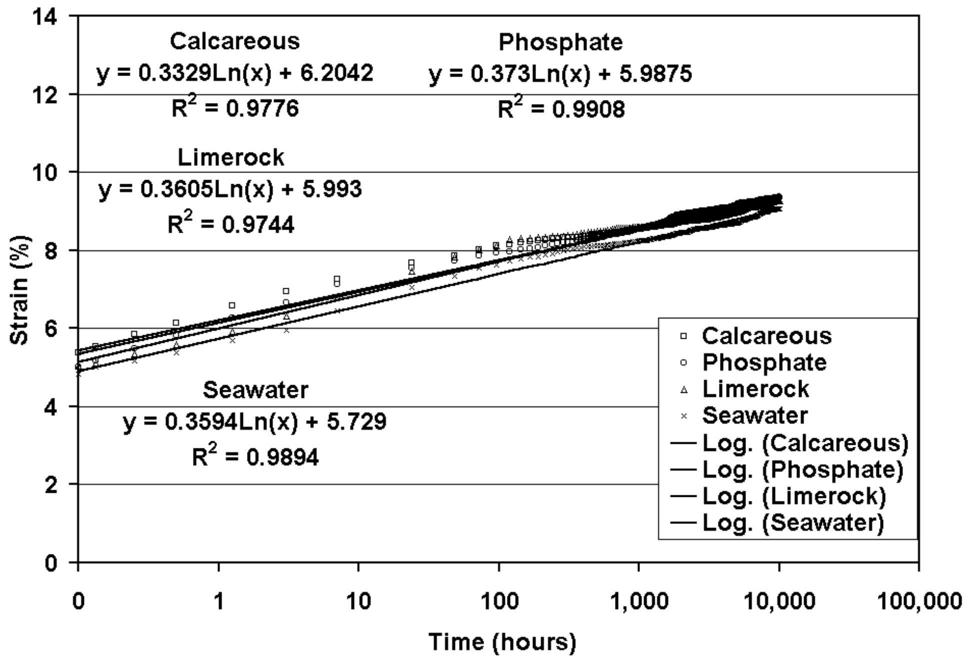

Figure 2. Creep curves for HDPE geogrids, T = 30°C, Load level = 30% ultimate load - Specimen set I

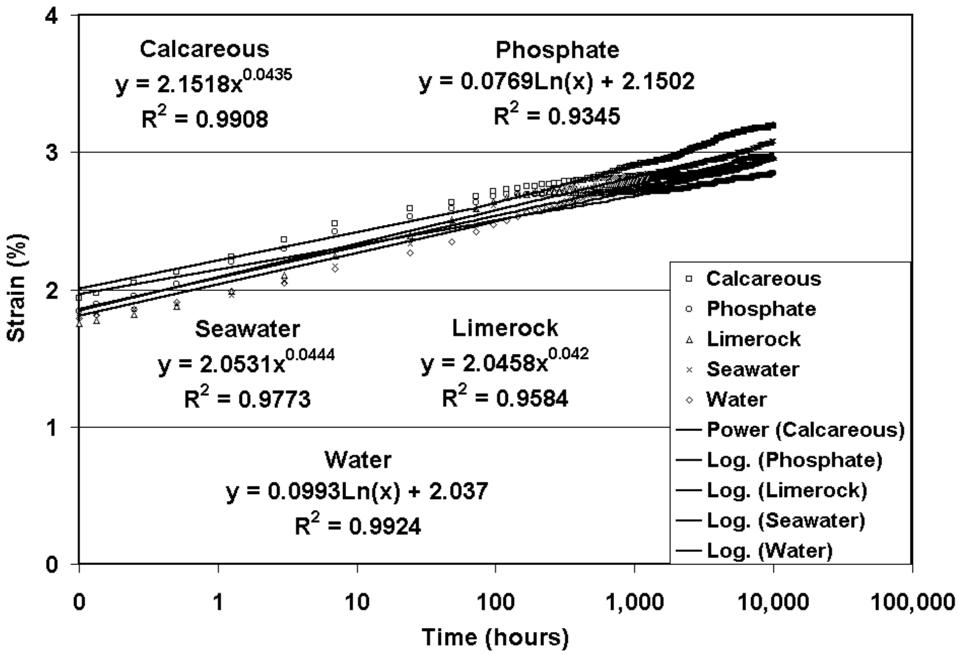

Figure 3. Creep curves for PET geogrids, T = 30°C, Load level = 30% ultimate load - Specimen set I

However, for both HDPE and PET specimens the increase in temperature and load level have a strong effect on the creep strain behavior, relatively larger for HDPE specimens.

It can be observed, that HDPE geogrids show large deformations, up to 55 % strain under the most extreme conditions (i.e. T= 65° C and Load level = 50% ultimate load, Figure 4), while for PET specimens the maximum strain was 14 % for the same conditions, Figure 5.

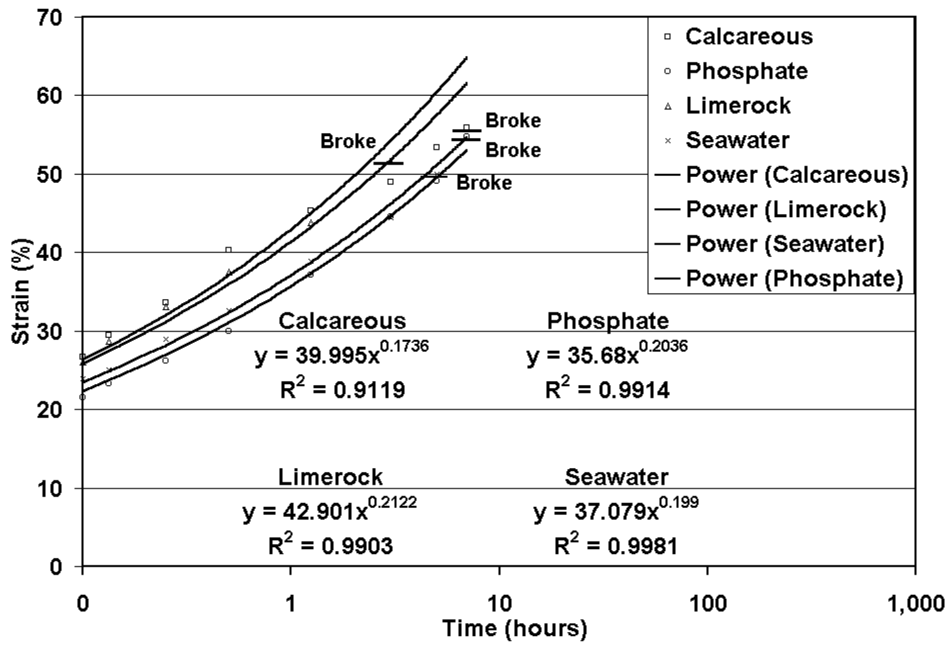

Figure 4. Creep curves for HDPE geogrids, T = 65°C, Load level = 50% ultimate load - Specimen set II

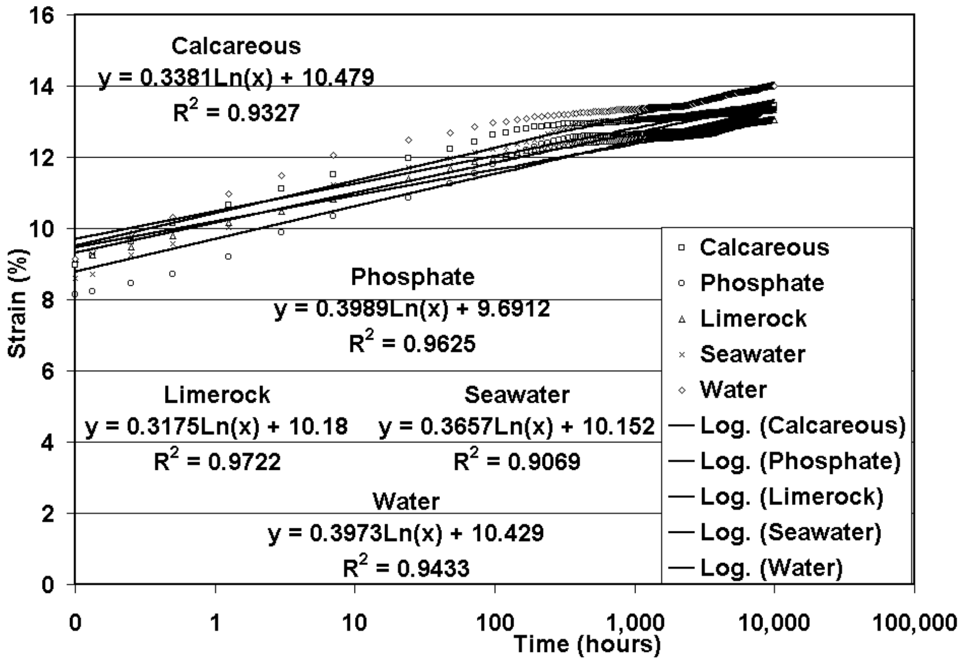

Figure 5. Creep curves for PET geogrids, T = 65°C, Load level = 50% ultimate load - Specimen set II

This shows that PET geogrids resist creep strain better than HDPE at similar temperatures and load levels.

From the results shown in Tables 1 to 4, it can be seen that the increase in temperature has a large influence on the amount of creep strain , and that specimens exposed to higher temperatures will be subjected to larger amounts of creep strain before breaking than those exposed to lower temperatures. Also, the creep strain at breaking for the HDPE specimens was about 50% when exposed to 55° C or 65° C. The increase in load level also increases the amount of creep strain in the specimens, but the influence is not as large as that due to the temperature. However, the higher the temperature, the larger is the influence of the increase in load level .

Table 1. Creep strain (%) for HDPE Specimens 30° C

Load level	30 %	40 %	50 %
Initial strain	4.5 - 5	4.5 - 6	7.5 - 8
Final strain	8.5 - 9	11 - 11.5	17.5 - 20.5

Table 2. Creep strain (%) for HDPE Specimens 45° C

Load level	30 %	40 %	50 %
Initial strain	6 - 6.5	8.6 - 9.5	11 -13
Final strain	10 - 11	16 - 19	34 - 39

Table 3. Creep strain (%) for HDPE Specimens 55° C

Load level	30 / %	40 / %	50 / %
Initial strain	6.3 - 7	9.5 - 10.5	14 -16
Final strain	10.5 - 11.5	23 - 27	46 - 53

Table 4. Creep strain (%) for HDPE Specimens 65° C

Load level	30 / %	40 / %	50 / %
Initial strain	8 - 9	11 - 13	19 -26
Final strain	17 - 19	28 - 33	46 - 56

From the results shown in Tables 5 to 8, it can be seen that the increase in temperature has a large influence on the amount of creep strain , but not as much as that encountered in HDPE specimens; for PET specimens the effects of temperature and load level are similar. It should be noticed that the different solutions do not seem to influence the amount of creep strain.

Table 5. Creep strain (%) for PET Specimens 30° C

Load level	30 / %	40 / %	50 / %
Initial strain	1.8 - 2.1	2.6 - 2.9	4.9 -5.3
Final strain	2.7 - 3.2	3.4 - 4	6.3 - 6.9

Table 6. Creep strain (%) for PET Specimens 45° C

Load level	30 / %	40 / %	50 / %
Initial strain	3.8 - 4.2	4 - 5	6.3 - 7
Final strain	5.2 - 5.9	5.6 - 6.5	8.4 - 9.8

Table 7. Creep strain (%) for PET Specimens 55° C

Load level	30 / %	40 / %	50 / %
Initial strain	3.6 - 4	5.2 - 5.8	7.8 - 8.2
Final strain	5..3 - 5.9	7.9 - 8.8	10.2 - 11

Table 8. Creep strain (%) for PET Specimens 65° C

Load level	30 / %	40 / %	50 / %
Initial strain	3.4 - 4.3	6.7 - 7.2	8.4 - 9
Final strain	6 - 6.6	9.2 - 10.2	13 -14

The PET specimens did not experience creep rupture except for two specimens, and for those two cases the rupture can be attributed to either defects in the specimens or poor clamping. On the other hand, for the HDPE specimens, creep rupture was observed in all the specimens exposed to 50% of the ultimate load; and for the 55° C and 65° C temperatures, creep rupture occurred at 40% of the ultimate load. Tables 9 to 11 show the time of rupture for the HDPE geogrids.

Table 9. Creep rupture for HDPE specimens load level = 50% ultimate load, T= 30° C & 45° C

Time/Strain	30° C-set I	30° C-set II	45° C-set I	45° C-set II
	Hours / %	Hours / %	Hours / %	Hours / %
Calcareous	8520 / 19.1	7752 / 18.9	528 / 39.1	408 / 35.4
Phosphate	6768 / 18.1	8040 / 19.7	408 /34.8	408 / 34.3
Limerock	3576 / 20.2	3696 / 17.5	408 / 38.7	480 / 37.4
Seawater	7584 / 19.5	6768 / 17.7	528 / 37	360 / 36.8

It can be observed in Table 9, that creep rupture occurred between 17.5 % and 20.2 % creep strain for the 30° C temperature and 50 % ultimate load, while for the 45° C temperature and 50% ultimate load the rupture occurred between 34.3 % and 39.1% creep strain . The rupture time for the 30° C temperature and 50 % ultimate load is between 6,768 and 8,520 hours, except for the limerock exposure, while for the 45° C temperature and 50% ultimate load, the time to rupture varied from 360 to 528 hours.

With these results it can be seen that the temperature has a strong effect on the percentage creep strain reached before creep rupture occurs and the time to creep rupture. The limerock exposure, at 30° C temperature and 50% ultimate load, reached creep rupture at only 3,576 to 3,696 hours. This can be attributed to non-uniform temperature exposure of the geogrid.

Table 10. Creep rupture for HDPE specimens load level = 50% ultimate load, T= 55° C & 65° C

Time/Strain	55° C-set I	55° C-set II	65° C-set I	65° C-set II
	Hours / %	Hours / %	Hours / %	Hours / %
Calcareous	120 / 46.2	48 / 52.5	5 / 46	7 / 55.9
Phosphate	120 / 51.2	120 / 50.3	5 /51.3	7 / 54.7
Limerock	96 / 51.5	96 / 52.2	7 / 48.4	3 / 51.7
Seawater	144 / 51.2	72 / 50.9	5 / 55.1	5 / 50

For the 55° C and 65° C temperatures, the percentage of creep strain before creep rupture does not vary significantly suggesting that the creep strain limit for the material has been reached. The time to reach creep rupture was further reduced with the increment in temperature.

From Table 11, it can be seen that for the 55° C temperature and 40% ultimate load, the percentage of strain before creep rupture was between 23.3% and 27 %, while for the 65°C temperature and 40% ultimate load it was between 29.6% and 32.7%, showing again that temperature affects the amount of creep strain reached before creep rupture.

Comparing Tables 10 and 11, it can be observed that the increase of load from 40% to 50% ultimate load also increases the creep strain before creep rupture.

It is clear from the results that the solution had no impact on the creep rupture, as the variabilities were principally from specimen to specimen. The only exception was limerock at 30° C temperature and 30% ultimate load. While this can be attributed to non-uniform distribution of temperature in the geogrid, which created regions, where the exposure temperature was higher than the 30° C required, not all the exposures indicated that to allow generalization.

Table 11. Creep rupture for HDPE specimens load level = 40% ultimate load, T= 55° C & 65° C

Time/Strain	55° C-set I	55° C-set II	65° C-set I	65° C-set II
	Hours / %	Hours / %	Hours / %	Hours / %
Calcareous	4392 / 23.3	2256 / 27	168 / 29.6	168 / 32.7
Phosphate	3576 / 23.5	3144 / 23.3	96 / 31	120 / 31.6
Limerock	3168 / 24.1	3432 / 24.2	168 / 31.7	168 /30.9
Seawater	2688 / 25.1	3192 / 23.6	240 / 29.9	240 / 30.2

3 CONCLUSIONS

In the creep plots, considerable variability of the data was encountered. This can be attributed to the testing of single rib specimens. The need to test more specimens for each condition has been identified. In the present research, it was not possible to test more than two specimens for each solution due to a large number of variables.

Regression analysis helped to address the variability and provide the equations to identify the creep strain at any given time. It can be observed that temperature and load have a strong effect on the creep behavior of HDPE geogrids. There is a large difference in creep strains between the HDPE geogrids exposed to 30° C and the ones exposed to 65° C, under the same load levels. Also, specimens exposed to higher temperatures showed a larger amount of creep strain before breaking, than those exposed to lower temperatures. Higher the temperature, the greater was the influence of increasing the load level. For PET specimens, the influence of temperature and load level is similar.

It is clear that HDPE geogrids undergo larger creep strain than PET geogrids. The different exposures do not play an important role in the rate of creep strain. It can be observed that there are larger variabilities from specimen to specimen, than from different solutions.

Creep rupture occurred in all the HDPE specimens exposed to 50% of the ultimate load. For the specimens exposed to 40% of the ultimate load, creep rupture occurred for specimens exposed to 55° C and 65° C temperatures. From the results, it was found that specimens exposed to similar loading, but higher temperatures, underwent larger deformations before creep rupture occurred, and the time to failure is reduced. Also, an increase of the load level produced an increase in the amount of creep strain reached before creep rupture occurred.

For the 55° C and 65° C temperatures, the percentage of creep strain before creep rupture did not vary significantly, indicating that the creep strain limit for the material has been reached. The time to reach creep rupture was further reduced with the increment in temperature.

The PET specimens did not experience creep rupture except for two specimens; for these two cases, the rupture can be attributed to either defects in the specimens or defective clamping.

ACKNOWLEDGEMENTS

This paper is based on a Florida Department of Transportation (FDOT)-funded project entitled "Strength and Durability of Backfill Geogrid for Retaining Walls", Work Program # 0510738. The authors are grateful to FDOT for the funding. The support and encouragement of Dr. S.E. Dunn, Professor and Chairman of the Department of Ocean Engineering, and Dr. J.T. Jurewicz, Dean of

Engineering, are gratefully acknowledged. Thanks are also due to Consejo Nacional de Ceiencia y Tecnologia (CONACYT) for its support to the second author (F. N.)

REFERENCES

Ahn, W. 1998. An Experimental and Analytical Investigation of Viscoelastic Pipe Soil Interaction, *Ph.D. Dissertation, Florida Atlantic University*, Boca Raton, Supervisor: Dr. D.V. Reddy, Florida DOT Research Contract Monitor: Powers, R. G

Allen, T. M. 1991. Determination of Long-Term Strength of Geosynthetics, *State-of-the-Art-Review, Proc., Geosynthetics 91 Conference*, Atlanta, USA. 351-379.

Allen, T. M., Bell, J. R., and Vinson T. S. 1983. Properties of Geotextiles in Cold Regions Applications, *Transportation Research Report No. 83-6*, Oregon State University, OR. USA.

ASTM D5265 1992 Standard Test Method for Evaluating the Unconfined Tension Creep Behavior of Geosynthetics, *Annual Book of ASTM Standards, Vol. 08 03.*

Koerner, M. R. et al. 1980. Stress Strain Time Behavior of Geotextiles in Uniaxial Tension, *Proc., Symposium on Geotextiles, ASCE*, Portland, OR, USA. 31-52.

McGrown, A., Andrews K. Z., and Kabir M. H. 1982 Load-Extension Testing of Geotextiles Confine In-Soil, *Second International Conference on Geotextiles Vol III*, Las Vegas, NV, USA. 793-798.

Reddy, D. V. 2000. Strength and Durability of Backfill Geogrid Reinforcement for Retaining Walls, *Report to FDOT*, Florida Atlantic University, Boca Raton, FL, USA.